nature geoscience

ARTICLES

PUBLISHED ONLINE: 21 MARCH 2016 | DOI: 10.1038/NGEO2681

Anthropogenic carbon release rate unprecedented during the past 66 million years

Richard E. Zeebe[1]*, Andy Ridgwell[2,3] and James C. Zachos[4]

Carbon release rates from anthropogenic sources reached a record high of ~10 Pg C yr^{-1} in 2014. Geologic analogues from past transient climate changes could provide invaluable constraints on the response of the climate system to such perturbations, but only if the associated carbon release rates can be reliably reconstructed. The Palaeocene–Eocene Thermal Maximum (PETM) is known at present to have the highest carbon release rates of the past 66 million years, but robust estimates of the initial rate and onset duration are hindered by uncertainties in age models. Here we introduce a new method to extract rates of change from a sedimentary record based on the relative timing of climate and carbon cycle changes, without the need for an age model. We apply this method to stable carbon and oxygen isotope records from the New Jersey shelf using time-series analysis and carbon cycle–climate modelling. We calculate that the initial carbon release during the onset of the PETM occurred over at least 4,000 years. This constrains the maximum sustained PETM carbon release rate to less than 1.1 Pg C yr^{-1}. We conclude that, given currently available records, the present anthropogenic carbon release rate is unprecedented during the past 66 million years. We suggest that such a 'no-analogue' state represents a fundamental challenge in constraining future climate projections. Also, future ecosystem disruptions are likely to exceed the relatively limited extinctions observed at the PETM.

As rapid reductions in anthropogenic carbon emissions[1] seem increasingly unlikely in the near future, forecasting the Earth system's response to ever-increasing emission rates has become a high-priority focus of climate research. Because climate model simulations and projections have large uncertainties—often due to the uncertain strength of feedbacks[2]—geologic analogues from past climate events are invaluable in understanding the impacts of massive carbon release on the Earth system[3,4]. The fastest known, massive carbon release throughout the Cenozoic (past 66 Myr) occurred at the onset of the Palaeocene–Eocene Thermal Maximum (~56 Myr ago; refs 5–9). The PETM was associated with a ~5 K surface temperature warming and an estimated total carbon release somewhere between current assessments of fossil fuel reserves (1,000–2,000 Pg C) and resources (~3,000–13,500 Pg C; refs 10,11). Although the PETM is widely considered the best analogue for present/future carbon release, the timescale of its onset, and hence the initial carbon release rate, have hitherto remained largely unconstrained. Determining the release rate is critical, however, if we are to draw future inferences from observed climate, ecosystem and ocean chemistry changes during the PETM (refs 3,7,8,12,13). If anthropogenic emissions rates have no analogue in Earth's recent history, then unforeseeable future responses of the climate system are possible.

Extracting rates without an age model

Carbon and oxygen isotope records ($\delta^{13}C$, $\delta^{18}O$) of the PETM exist for various marine sections spanning pelagic to shallow marine depositional environments. Pelagic records have robust stratigraphic control, but, given relatively slow sedimentation rates and carbonate dissolution, lack the fidelity required to assess the rate of the carbon isotope excursion (CIE) onset[14,15]. The most expanded marine records are found in shelf siliciclastic settings, where sedimentation rates are as much as ten times higher and the effects of carbonate dissolution are minimal[16]. Despite the lack of accurate stratigraphic age control, these records have the greatest potential to resolve the relative phasing between carbon cycle and climate changes.

Our advance here is to recognize that an age model is not strictly necessary to extract rates of change from the geologic record. Critically, whereas $\delta^{13}C$ tracks the timing of the carbon release, $\delta^{18}O$ tracks the climate response to CO_2 and other forcings. The climate response is not instantaneous, but rather shows a characteristic temporal delay depending on the climate system's thermal inertia[17–19]. For instance, the rate at which Earth's surface temperature approaches a new equilibrium depends critically on the ocean's heat uptake efficiency. Whereas the initial few percent of the response may be achieved within decades, the final few percent can take up to millennia. Thus, the absence of a detectable lag between $\delta^{13}C$ and $\delta^{18}O$ in any high-fidelity record spanning the PETM onset requires that the onset occurred more slowly than some threshold. Otherwise, if, for example, the carbon release was very rapid, $\delta^{18}O$ would substantially lag behind $\delta^{13}C$. The threshold can be determined as a function of the characteristic response time of the climate system and the specific nature of the isotope records and their associated uncertainty ('noise'), as detailed below. We emphasize that our approach is by no means restricted to the PETM onset, and may be applied to other past climate perturbations, given high-resolution isotope records and a proper timescale of climate–carbon cycle changes.

Several possible candidate records with high sedimentation rates exist from the subsiding continental margin of the US east coast[16,20,21] (Fig. 1). However, at present only one section, from Millville,

[1]School of Ocean and Earth Science and Technology, University of Hawaii at Manoa, 1000 Pope Road, MSB 629, Honolulu, Hawaii 96822, USA. [2]School of Geographical Sciences, University of Bristol, University Road, Bristol BS8 1SS, UK. [3]Department of Earth Sciences, University of California Riverside, 900 University Avenue, Riverside, California 92521, USA. [4]Earth and Planetary Sciences, University of California Santa Cruz, 1156 High Street, Santa Cruz, California 95064, USA. *e-mail: zeebe@soest.hawaii.edu

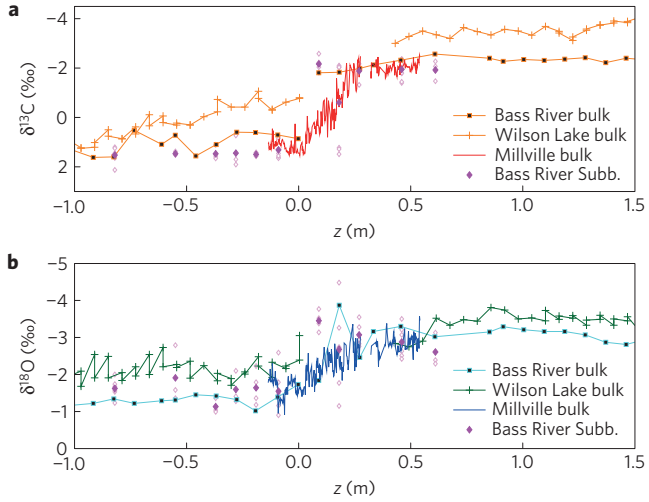

Figure 1 | Selected stable isotope records from New Jersey margin sections across the PETM onset[16,20,21,23]. **a**,**b**, Carbon ($\delta^{13}C$) (**a**) and oxygen ($\delta^{18}O$) (**b**) isotopes plotted versus position in core (the $z = 0$ m alignment is arbitrary). Also, in the depth domain, the length of the onset interval cannot be compared between locations because of different sedimentation rates. Subb., species of *Subbotina* (planktonic foraminifer). Open (filled) diamonds indicate all (mean) Subb. values. Note that the Millville bulk isotope records are consistent with data from planktonic foraminifera at the same site[22].

New Jersey, has cm-resolution bulk isotope records (foraminiferal isotopes at lower resolution)[22], potentially offering the highest-fidelity recording of the onset[23,24] (Fig. 2). Although we use isotope records of bulk carbonate below that may have an unknown diagenetic overprint (see Supplementary Information), we argue that the relative sense and timing of change between $\delta^{13}C$ and $\delta^{18}O$ during the PETM onset has been retained. Indeed, both the ~3‰ CIE across the onset and the concomitant ~1‰ $\delta^{18}O$-drop at Millville (indicating ~5 K warming) are consistent with most other pelagic sequences[9] and foraminifer isotope data from nearby sections at Bass River[20] and Wilson Lake[21,25] (Fig. 1). Most importantly, the Millville bulk isotope records are consistent with data from planktonic foraminifera at the same site[22], which lends confidence in our approach, as foraminifera are considered robust recorders of changes in $\delta^{13}C$ and $\delta^{18}O$. For further discussion of the Millville records, including spectral analysis, bioturbation, couplets and contamination, see Supplementary Information. We emphasize that the resolution of other PETM sections across the onset (including at Bass River and Wilson Lake) is insufficient at present to determine leads and lags between $\delta^{13}C$ and $\delta^{18}O$. We hence use the Millville record as the target for our approach and derive an estimate for the maximum rate of carbon release across the PETM onset.

First, we determine possible $\delta^{13}C$–$\delta^{18}O$ leads/lags in the Millville records (depth domain). Then we simulate carbon release ($\delta^{13}C$) and climate response ($\simeq\delta^{18}O$) using carbon cycle/climate models, while varying the carbon release time. The fastest possible release that still yields leads/lags consistent with the data will provide the minimum time interval for the PETM onset.

Leads and lags

We determined potential leads/lags between the $\delta^{13}C$ and $\delta^{18}O$ Millville records for the non-stationary and (transformed) stationary time series (Fig. 2). For the former, we focus on obvious leads/lags at the onset's start- and endpoint. The gap at $z = 0.41$–0.46 m ($\%CaCO_3 < 0.1\%$) prevents any lead/lag determination at the onset's endpoint. Zooming in on the start,

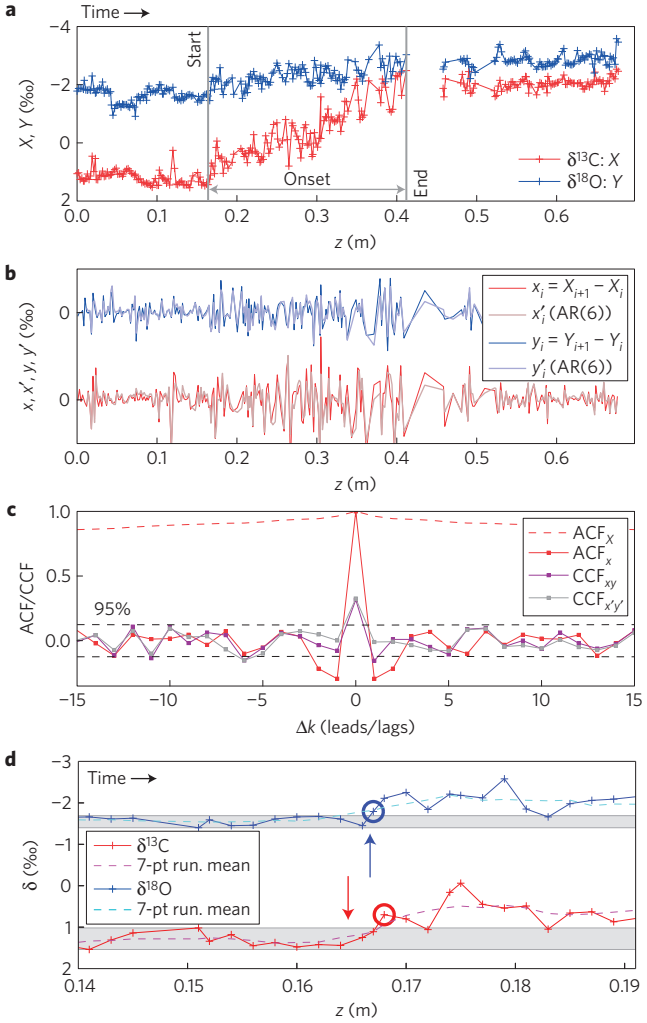

Figure 2 | Millville PETM records and time-series analysis. **a**, Bulk stable carbon and oxygen isotopes (X, $\delta^{13}C$; Y, $\delta^{18}O$). Time runs to the right (oldest sample was assigned depth $z = 0$ m). **b**, First-order differenced time series (x,y) and pre-whitened (filtered) series (x',y'). See text for details. AR(6), autoregressive process of order six (see Supplementary Information). **c**, Leads/lags based on autocorrelation function (ACF) and cross-correlation function (CCF). Dashed horizontal lines, 95% confidence interval ($\sim\pm2/\sqrt{N}\simeq0.12$; N, number of data points in the time series). After pre-whitening, $CCF_{x'y'}$ (grey squares) shows significant correlation only at $\Delta k = 0$ (contemporaneous) and at $\Delta k = -6$ (see text). **d**, Leads/lags between Millville $\delta^{13}C$ (red) and $\delta^{18}O$ (blue) at the start of the PETM onset. Arrows, apparent start based on superficial visual inspection; grey bars, range of pre-onset variability. Circles, first onset samples exceeding pre-onset variability; dashed lines, seven-point running means.

$\delta^{13}C$ apparently leads $\delta^{18}O$ by one sample step in the depth domain ($\Delta k = +1$, Fig. 2d, arrows). However, considering the immediate pre-onset variability, onset $\delta^{13}C$ and $\delta^{18}O$ values exceed the minimum pre-onset values at only three and one samples above the apparent onset, respectively, indicating a $\delta^{13}C$-lag by one sample step ($\Delta k = -1$, Fig. 2d, circles). Seven-point running mean curves (compared to maximum pre-onset values) would also indicate a slight $\delta^{13}C$-lag relative to $\delta^{18}O$. Altogether, we take $\Delta k = \pm2$ as an estimated upper limit for possible leads/lags between the non-stationary time series.

We also determined possible systematic leads/lags across the full records using time-series analysis. The raw data series ($X = \delta^{13}C$, $Y = \delta^{18}O$) are non-stationary and inadequate for

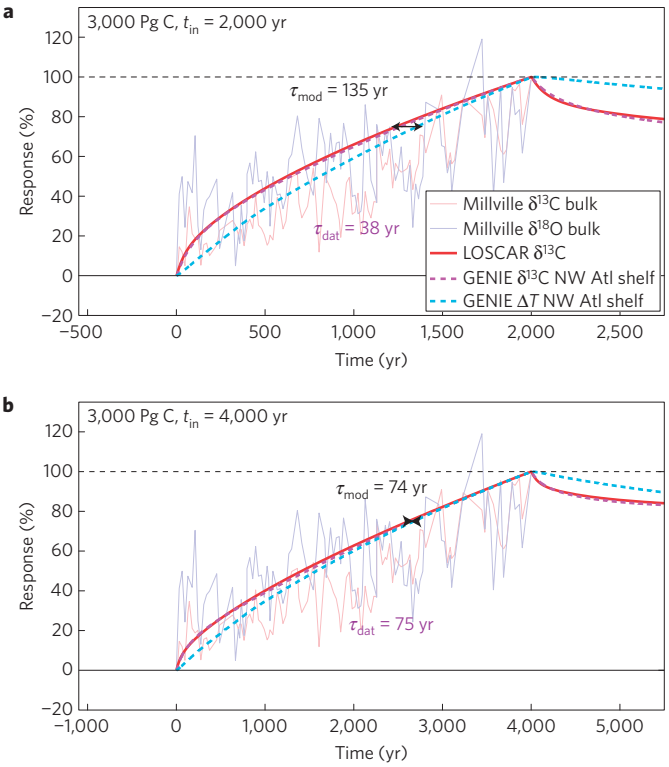

Figure 3 | Examples of model time lags (τ_{mod}) as a function of model release time (t_{in}). a,b, Lags are plotted for $t_{in} = 2{,}000$ yr (**a**) and $t_{in} = 4{,}000$ yr (**b**). $\tau_{dat} = 2\Delta z/\bar{r}_{sed}$ indicates the maximum lead/lag allowed by the time-series analysis of the data records (see text). Note different time axes. All records and model output are normalized to % response. Simulated δ^{13}C leads the model climate response at the onset's start because the models are forced by carbon input. In reality, temperature may have led carbon input initially[5,31], although the data do not support any significant δ^{18}O lead at the start (Fig. 2d). Nevertheless, to avoid potential model bias during the initial onset phase, we determine τ_{mod} (arrows) as an average model lag, omitting the initial 40% of the normalized response (see Supplementary Information). The scenario shown in **a** is not feasible as τ_{mod} substantially exceeds τ_{dat}. Note that τ_{dat} is not to be determined from the raw (non-stationary) data records but from the first-order differenced and pre-whitened time series using cross-correlation (see text and Supplementary Information).

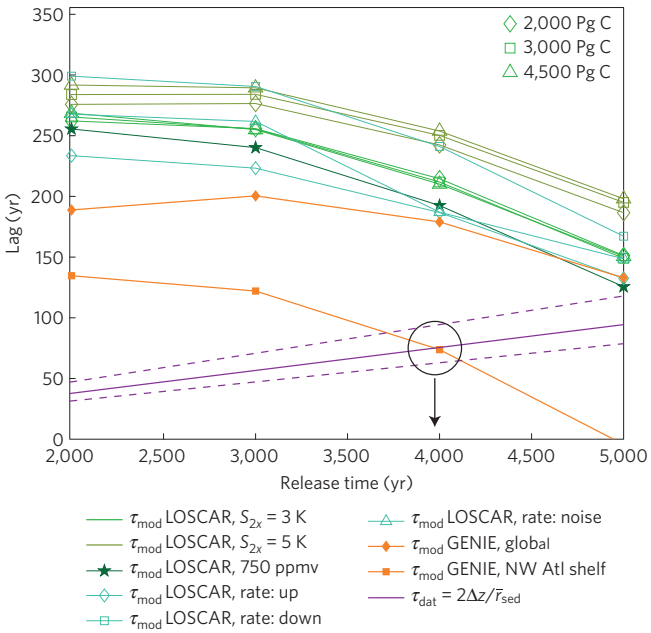

Figure 4 | Determining the minimum release time. Maximum lead/lag is based on data records (τ_{dat}) and model time lag (τ_{mod}) calculated using carbon cycle/climate models GENIE (ref. 12) and LOSCAR (refs 29,30), see text. The intercept of the shortest τ_{mod} and τ_{dat} yields the minimum onset interval consistent with the data (~4,000 yr, black circle and arrow). The dashed purple lines illustrate potential uncertainties in τ_{dat} from variations in the onset length in the Millville core ($z_{in} \pm 20\%$; however, see text and Supplementary Information). Standard model runs use 3,000 Pg C carbon input and climate sensitivity $S_{2\times} = 3$ K per CO_2 doubling. Sensitivity of τ_{mod} was tested by varying the model release time (horizontal axis), total carbon input (open symbols: 2,000, 3,000, and 4,500 Pg C), carbon release patterns (rate: up, down, noise), climate sensitivity ($S_{2\times}$), initial (pre-event) pCO_2 (750–1,000 ppmv), and atmospheric versus deep-ocean carbon injection (see Supplementary Information). NW Atl shelf represents GENIE grid-point output on the northwest Atlantic shelf corresponding to Millville's palaeo-location (see Supplementary Information).

determining leads/lags based on autocorrelation function (ACF) and cross-correlation function (CCF; refs 26,27). Thus, we use first-order differencing:

$$x_i = X_{i+1} - X_i; \quad y_i = Y_{i+1} - Y_i \tag{1}$$

The ACFs of the differenced series (Fig. 2) are similar to white-noise ACFs, except for significant negative correlations (95% level) at $\Delta k = \pm 1, \pm 2$, which can lead to spurious correlations in the CCF (refs 26–28).

Indeed, CCF_{xy} shows a significant negative correlation at $\Delta k = +1$, which, however, disappears after pre-whitening (series x', y', Supplementary Information). The single large peak in $CCF_{x'y'}$ at $\Delta k = 0$ indicates a contemporaneous relationship. The correlation at $\Delta k = -6$ is barely significant and, in fact, 5 out of 100 (or 1/20) 'significant' correlations are expected at the 95% confidence level even if the series are truly random. Moreover, the correlation is negative, which is not relevant for a potential causal relationship between δ^{13}C and δ^{18}O (or vice versa) during carbon release and warming. Such a relationship requires a positive correlation—that is, deviations towards lighter values in both records. Thus, within the limits of the data resolution (average Δz), we find a significant contemporaneous correlation ($\Delta k = 0$) but can not detect any significant leads/lags between the stationary series (full records). The same holds true for the stationary sub-series that cover only the onset or parts of it (Supplementary Information). We conclude from the combined stationary and non-stationary analyses that $|\Delta k| \leq 2$ for possible leads/lags between the Millville δ^{13}C and δ^{18}O records.

Carbon cycle–climate modelling

The maximum lead/lag derived from the data records (τ_{dat}) provides a strong constraint for the carbon cycle/climate models in determining the minimum onset interval. Given a total carbon input and a model release time, the simulated lag (τ_{mod}) between surface temperature ($\simeq\delta^{18}$O) and δ^{13}C must not exceed τ_{dat} (time domain) at lag $= \max|\Delta k| \times \Delta z$ in the depth domain:

$$\tau_{mod} \leq \tau_{dat} = \max|\Delta k| \Delta z/\bar{r}_{sed} \tag{2}$$

where $\Delta z = 0.234$ cm is the average sampling resolution across the onset and $\max|\Delta k| = 2$ (see above). Furthermore, $\bar{r}_{sed} = z_{in}/t_{in}$ (to be determined) represents an average sedimentation rate, where $z_{in} = 24.8$ cm is the onset interval in the Millville core (Fig. 2a) and t_{in} is the model release time. Importantly, $r_{sed}(t)$ does not need to be constant for our approach (see Supplementary

Information). The final calculated $\bar{r}_{sed} \simeq 6$ cm kyr^{-1} during the onset (see below) is consistent with foraminifer accumulation rates[24] and falls between rates within the basal PETM section at Bass River[21] (2.8 cm kyr^{-1}) and average PETM rates at Wilson Lake/Bass River[21] (10–20 cm kyr^{-1}).

Although τ_{dat} is not known a priori without a robust age model, we can quantify τ_{mod} (and hence constrain the minimum value of τ_{dat}, equation (2)) using the carbon cycle/climate models GENIE (ref. 12) and LOSCAR (refs 29,30) (Fig. 3). Note that lead–lag determination using cross-correlation is unsuitable for the model output. Model leads/lags were directly determined from the normalized response (see Supplementary Information). In addition to global mean sea surface temperature (SST) and $\delta^{13}C$, we analysed GENIE's grid-point output on the northwest Atlantic shelf (NW Atl shelf, corresponding to Millville's palaeo-location, see Supplementary Information). For instance, at 3,000 Pg C (varied below) released over 2,000 yr, the SST response (ΔT) lags substantially behind model-$\delta^{13}C$ ($\tau_{mod} \simeq 135$ yr, see Fig. 3a). In contrast, equation (2) gives τ_{dat} of only 38 yr at $t_{in} = 2{,}000$ yr. At 3,000 Pg C input, GENIE's τ_{mod} on the NW Atl shelf approaches τ_{dat} only for input times $\gtrsim 4{,}000$ yr (Figs 3 and 4).

To evaluate the sensitivity of the calculated minimum onset interval to critical parameters, we varied the model release time, release pattern, total carbon input (2,000, 3,000, 4,500 Pg C), climate sensitivity, initial (pre-event) pCO_2 (Fig. 4), and atmospheric versus deep-ocean carbon injection (Supplementary Information). (Note that for long release times, τ_{mod} reverses sign—that is, SST starts leading $\delta^{13}C$, see Supplementary Information.) Also, simulated $\delta^{13}C$ leads the model climate response at the onset's start because the models are forced by carbon input. In reality, temperature may have led carbon input initially[5,31], although the data do not support any significant $\delta^{18}O$-lead at the start (Fig. 2d). Nevertheless, we consider this potential bias when determining model time lags (Supplementary Information). GENIE's NW Atl shelf response indeed represents the shortest τ_{mod} of all scenarios tested. The intercept of the shortest τ_{mod} and τ_{dat} yields the minimum onset interval consistent with the data, namely ~4,000 yr (Fig. 4).

Data uncertainties and implications

Our analysis yields an average sedimentation rate of 6.2 cm kyr^{-1} at $t_{in} = 4{,}000$ yr, and thus an average sampling resolution of ~40 years, at Millville. Hence we cannot rule out brief pulses of carbon input above average rates on timescales $\lesssim 40$ yr (a similar limitation arises from time averaging of the primary signal in sediments). However, if such pulses occurred, their contribution to the maximum sustained rate must have been small. Otherwise, $\delta^{13}C$ would show large, rapid step-like drops following such pulses, which is not the case (Fig. 2a). Our results do not support a two-step carbon release[32], for which the effect of bioturbation and mixing with our estimated sedimentation rate at Millville would only damp, not obliterate, a prominent $\delta^{13}C$ reversal midway through the onset. We note that a previous study determined leads/lags between climatic/biotic events at one PETM site[33]. However, the data and model results were not used to constrain the time interval of the onset. Most importantly, the simulation assumed instantaneous carbon release—unsuitable for our approach.

We also consider that the end of the onset interval at Millville could be located within the gap at $z = 0.41$–0.46 m (%$CaCO_3$ <0.1%, Fig. 2). If the onset-end occurred at 0.46 m (20% larger z_{in} for a given t_{in}), the average sedimentation rate would be higher and τ_{dat} smaller (equation (2)). For a smaller τ_{dat}, the intercept with τ_{mod} occurs later (Fig. 4), which would give a longer duration for the calculated onset interval. Although it is unlikely that z_{in} was initially smaller and subsequently smoothed/expanded, for example, by bioturbation (Supplementary Information), we also illustrate the effect of a 20% smaller z_{in} on τ_{dat} (Fig. 4).

The initial carbon release during the PETM onset thus occurred over at least 4,000 yr. Using estimates of 2,500–4,500 Pg C for the initial carbon release, the maximum sustained PETM carbon release rate was therefore 0.6–1.1 Pg C yr^{-1}. Given currently available palaeorecords, we conclude that the present anthropogenic carbon release rate (~10 Pg C yr^{-1}) is unprecedented during the Cenozoic (past 66 Myr). Possible known consequences of the rapid man-made carbon emissions have been extensively discussed elsewhere[2,30,34,35]. Regarding impacts on ecosystems, the present/future rate of climate change and ocean acidification[12,36,37] is too fast for many species to adapt[38], which is likely to result in widespread future extinctions in marine and terrestrial environments that will substantially exceed those at the PETM (ref. 13). Given that the current rate of carbon release is unprecedented throughout the Cenozoic, we have effectively entered an era of a no-analogue state, which represents a fundamental challenge to constraining future climate projections.

Code availability

The C code for the LOSCAR model can be obtained from the author (R.E.Z.) upon request.

Received 23 October 2015; accepted 19 February 2016; published online 21 March 2016

References

1. Le Quéré, C. *et al*. Global carbon budget 2015. *Earth Syst. Sci. Data* **7,** 349–396 (2015).
2. IPCC *Climate Change 2013: The Physical Science Basis* (eds Stocker, T. F. *et al*.) (Cambridge Univ. Press, 2013).
3. Zachos, J. C., Dickens, G. R. & Zeebe, R. E. An early Cenozoic perspective on greenhouse warming and carbon-cycle dynamics. *Nature* **451,** 279–283 (2008).
4. Rohling, E. J. *et al*. Making sense of palaeoclimate sensitivity. *Nature* **491,** 683–691 (2012).
5. Dickens, G. R., O'Neil, J. R., Rea, D. K. & Owen, R. M. Dissociation of oceanic methane hydrate as a cause of the carbon isotope excursion at the end of the Paleocene. *Paleoceanography* **10,** 965–971 (1995).
6. Zachos, J. C., Pagani, M., Sloan, L., Thomas, E. & Billups, K. Trends, rhythms, and aberrations in global climate 65 Ma to present. *Science* **292,** 686–693 (2001).
7. Zachos, J. C. *et al*. Rapid acidification of the ocean during the Paleocene–Eocene Thermal Maximum. *Science* **308,** 1611–1615 (2005).
8. Zeebe, R. E., Zachos, J. C. & Dickens, G. R. Carbon dioxide forcing alone insufficient to explain Palaeocene-Eocene Thermal Maximum warming. *Nature Geosci.* **2,** 576–580 (2009).
9. McInerney, F. A. & Wing, S. L. The Paleocene–Eocene Thermal Maximum: a perturbation of carbon cycle, climate, and biosphere with implications for the future. *Annu. Rev. Earth Planet. Sci.* **39,** 489–516 (2011).
10. Rogner, H. An assessment of world hydrocarbon resources. *Annu. Rev. Energy Environ.* **22,** 217–262 (1997).
11. McGlade, C. & Ekins, P. The geographical distribution of fossil fuels unused when limiting global warming to 2 °C. *Nature* **517,** 187–190 (2015).
12. Ridgwell, A. & Schmidt, D. Past constraints on the vulnerability of marine calcifiers to massive carbon dioxide release. *Nature Geosci.* **3,** 196–200 (2010).
13. Zeebe, R. E. & Zachos, J. C. Long-term legacy of massive carbon input to the Earth system: Anthropocene vs. Eocene. *Phil. Trans. R. Soc. A* **371,** 20120006 (2013).
14. Farley, K. A. & Eltgroth, S. F. An alternative age model for the Paleocene-Eocene thermal maximum using extraterrestrial ^{3}He. *Earth Planet. Sci. Lett.* **208,** 135–148 (2003).
15. Murphy, B. H., Farley, K. A. & Zachos, J. C. An extraterrestrial ^{3}He-based timescale for the Paleocene-Eocene thermal maximum (PETM) from Walvis Ridge, IODP Site 1266. *Geochim. Cosmochim. Acta* **74,** 5098–5108 (2010).
16. John, C. M. *et al*. North American continental margin records of the Paleocene-Eocene thermal maximum: implications for global carbon and hydrological cycling. *Paleoceanography* **23,** PA2217 (2008).
17. Hansen, J. *et al*. Climate response times: dependence on climate sensitivity and ocean mixing. *Science* **229,** 857–859 (1985).
18. Roe, G. Feedbacks, timescales, and seeing red. *Annu. Rev. Earth Planet. Sci.* **37,** 93–115 (2009).
19. Hansen, J., Sato, M., Kharecha, P. & von Schuckmann, K. Earth's energy imbalance and implications. *Atmos. Chem. Phys.* **11,** 13421–13449 (2011).

20. Zachos, J. C. *et al*. The Paleocene-Eocene carbon isotope excursion: constraints from individual shell planktonic foraminifer records. *Phil. Trans. R. Soc. A* **365,** 1829–1842 (2007).
21. Stassen, P., Thomas, E. & Speijer, R. P. Integrated stratigraphy of the Paleocene-Eocene thermal maximum in the New Jersey Coastal Plain: toward understanding the effects of global warming in a shelf environment. *Paleoceanography* **27,** PA4210 (2012).
22. Makarova, M., Miller, K. G., Wright, J. D., Rosenthal, Y. & Babila, T. Temperature and salinity changes associated with the Paleocene-Eocene Carbon Isotope Excursion along the mid Atlantic margin. AGU Fall Meeting abstr. PP33C–2322 (2015).
23. Wright, J. D. & Schaller, M. F. Evidence for a rapid release of carbon at the Paleocene-Eocene thermal maximum. *Proc. Natl Acad. Sci. USA* **110,** 15908–15913 (2013).
24. Pearson, P. N. & Thomas, E. Drilling disturbance and constraints on the onset of the Paleocene-Eocene boundary carbon isotope excursion in New Jersey. *Clim. Past* **11,** 95–104 (2015).
25. Zachos, J. C. *et al*. Extreme warming of mid-latitude coastal ocean during the Paleocene–Eocene Thermal Maximum: inferences from TEX_{86} and isotope data. *Geology* **34,** 737–740 (2006).
26. Wei, W. W. S. *Time Series Analysis: Inivariate and Multivariate Methods* (Addison-Wesley, 1990).
27. Chatfield, C. *The Analysis of Time Series: An Introduction* 6th edn (CRC Press, 2004).
28. Box, G. E. P. & Jenkins, G. M. *Time Series Analysis: Forecasting and Control* (Holden-Day, 1970).
29. Zeebe, R. E. LOSCAR: long-term ocean-atmosphere-sediment carbon cycle reservoir model v2.0.4. *Geosci. Model Dev.* **5,** 149–166 (2012).
30. Zeebe, R. E. Time-dependent climate sensitivity and the legacy of anthropogenic greenhouse gas emissions. *Proc. Natl Acad. Sci. USA* **110,** 13739–13744 (2013).
31. Sluijs, A. *et al*. Environmental precursors to rapid light carbon injection at the Palaeocene/Eocene boundary. *Nature* **450,** 1218–1221 (2007).
32. Bowen, G. J. *et al*. Two massive, rapid releases of carbon during the onset of the Palaeocene-Eocene thermal maximum. *Nature Geosci.* **8,** 44–47 (2015).
33. Bralower, T. J., Meissner, K. J., Alexander, K. & Thomas, D. J. The dynamics of global change at the Paleocene-Eocene thermal maximum: a data-model comparison. *Geochem. Geophys. Geosyst.* **15,** 3830–3848 (2014).
34. National Research Council *Abrupt Impacts of Climate Change: Anticipating Surprises* (The National Academies Press, 2013).
35. Robinson, A., Calov, R. & Ganopolski, A. Multistability and critical thresholds of the Greenland ice sheet. *Nature Clim. Change* **2,** 429–432 (2012).
36. Caldeira, K. & Wickett, M. E. Anthropogenic carbon and ocean pH. *Nature* **425,** 365 (2003).
37. Zeebe, R. E., Zachos, J. C., Caldeira, K. & Tyrrell, T. Oceans: carbon emissions and acidification (in perspectives). *Science* **321,** 51–52 (2008).
38. Rockström, J. *et al*. A safe operating space for humanity. *Nature* **461,** 472–475 (2009).

Acknowledgements

We thank E. Thomas for sharing data and G. Bowen for discussions. We gratefully acknowledge the NO.COM.ET project. This research was supported by NSF grant OCE12-20602 to J.C.Z. and R.E.Z. and EU grant ERC-2013-CoG-617313 to A.R.

Author contributions

R.E.Z. led the effort. All authors wrote the paper.

Additional information

Supplementary information is available in the online version of the paper. Reprints and permissions information is available online at www.nature.com/reprints. Correspondence and requests for materials should be addressed to R.E.Z.

Competing financial interests

The authors declare no competing financial interests.